Journal of Applied Electrochemistry (2006) 36:255–264
DOI 10.1007/s10800-005-9066-y

Alkaline peroxide generation using a novel perforated bipole trickle-bed electrochemical reactor

NEERAJ GUPTA* and COLIN W. OLOMAN
*Department of Chemical & Biological Engineering, University of British Columbia, Vancouver, BC V6T1Z4, Canada (*author for correspondence, e-mail: neeraj.gupta@nrc-cnrc.gc.ca)*

Received 6 May 2005; accepted in revised form 2 September 2005

Key words: electrochemical, electro-reduction, electro-synthesis, 3D electrodes, graphite felt, oxygen, perforated bipole, peroxide, trickle-bed

Abstract

A novel perforated bipole trickle-bed electrochemical reactor is investigated for the electro-synthesis of alkaline peroxide. The process uses a relatively simple cell configuration in which a single electrolyte flows with oxygen gas in a flow-by graphite felt cathode, sandwiched between a micro-porous diaphragm and a perforated bipolar electrode plate. The graphite felt cathodes are 120 mm high by 25 mm wide and have a thickness of 3.2 mm. The reactor is operated at current densities in the range 1–5 kA m^{-2}, ca. 800 kPa (abs) pressure and temperature (In/Out) 20–45 °C with one and two-cells. The reactor shows good performance (current efficiency ~78% at 2 kA m^{-2} and a specific energy of 5 kWh per kg of peroxide generated) with peroxide concentrations from 0.02 to 0.15 M in 1 M NaOH.

1. Introduction

The electro-reduction of oxygen to peroxide has been known since the 19th century [1] and in the last 30 years has had special attention in respect to the electro-synthesis of alkaline peroxide solutions for bleaching wood pulp [2, 3].

Practical continuous reactors for the electro-synthesis of alkaline peroxide must use cathode materials (such as carbon) that are electrochemically selective for oxygen reduction to peroxide over hydroxide, in three-dimensional (3D) configuration to cope with the mass transfer constraint imposed by the low solubility of oxygen in aqueous electrolytes (ca. 1 mM at STP). The configuration of these cathodes was reviewed by Foller and Bombard in 1995 [4] and ranges from the gas-diffusion electrode first described by Berl [5] and subsequently elaborated by Foller [6], Drackett [7] and others, to the trickle-bed electrode introduced by Oloman and Watkinson [8] and developed to a commercial process in the mono-polar diaphragm-flow control trickle-bed cell of H-D Tech Inc. [9, 10].

Due to their complexity and/or low current density each of the electrochemical peroxide reactors implicated above has a high capital cost that compromises its competitive position with the established thermo-chemical process of cyclic hydrogenation and oxygenation of alkyl anthraquinones. For example, the relatively complex oxygen gas-diffusion cathodes developed by E-TEK (and others) operate near atmospheric pressure at superficial current density up to about 2.5 kA m^{-2}, whereas the simpler H-D Tech trickle-bed cathodes run at superficial current densities up to about 1 kA m^{-2}. In both cases the amortized capital cost of the reactors per unit of peroxide product is a large fraction of the market price of hydrogen peroxide, which is currently US$ 1.5/kg (US$ 0.48/lb 70%$_w$ H_2O_2) including freight charges [11].

Since 1995 notable publications on the electro-synthesis of alkaline peroxide include those of Sudoh et al. who did experimental, modeling and scale-up work with trickle-bed cathodes of graphite felt [12, 13]. A detailed summary of this and other work on alkaline peroxide up to 2004 has been presented by Gupta [14].

Graphite felt trickle-bed cathodes have also been the subject of substantial work at U.B.C., where the gas to solid mass transfer capacity in such two-phase flow-by electrodes was measured up to 9 s^{-1} [15]. This high mass transfer capacity opens the door to carrying out the electro-reduction of oxygen to peroxide under super-atmospheric oxygen pressure (e.g. 1000 kPa (abs)) at superficial effective current densities up to about 5 kA m^{-2}. The properties of graphite felt, coupled with the stoichiometry of alkaline peroxide electro-synthesis, allows the concept of a simple (i.e. low capital cost) multi-cell bipolar reactor in which each cell consists of a porous diaphragm pressed between a 3D cathode and a bipole plate that is perforated to allow the oxygen gas generated at the anode to flow directly into the adjacent cathode [16]. The viability of such a perforated bipole reactor hinges on the possibility of suppressing internal current by-pass through manipulating the perforation coverage and operating under conditions that keep the

perforations loaded with gas. A 10-cell (0.4 m^2/cell) perforated bipole reactor was demonstrated at U.B.C. in the 1980s, to generate alkaline peroxide (2 wt% H_2O_2 in 6 wt% NaOH) under 800 kPa (abs) oxygen pressure at 60 °C, with superficial current densities up to 2.5 kA m^{-2}/2 V per cell at 75% peroxide current efficiency (cf. Appendix) and specific energy electrical energy consumption of 4.2 kWh kg^{-1} H_2O_2 [3]. This previous work on the perforated bipole reactor was carried out under a commercial contract and no detailed study of the reactor has been published to date.

The economics of the U.B.C. process is a trade-off between capital and operating costs. Operating the electrochemical reactor at high current densities lowers the capital cost due to lower surface area of the electrodes, whereas working at low current densities decreases the operating cost (specific electrical energy consumption) due to higher peroxide efficiencies. A detailed economic analysis of the present process has been described elsewhere [14].

The present paper details the perforated bipole reactor and gives the results of preliminary experimental work aimed at the design, modeling, scale-up and economic analysis of this novel multi-cell electrochemical reactor for the production of alkaline peroxide solutions [14].

2. Reactor concept

Table 1 summarizes the reactions that occur in the synthesis of alkaline peroxide in an electrochemical cell with a porous diaphragm separator.

Perhydroxyl ions are generated on the cathode by reaction 1 and reduced to hydroxyl ions by reaction 2. Reaction 1 is kinetically favored on carbon over reaction 2 by about two orders of magnitude [17], so that perhydroxyl ions accumulate with high selectivity in a graphite felt cathode operating a sub-limiting current density for reaction 1. A few other materials, such as gold, mercury, some transition metal oxides and metal complexes are also selective for peroxide [17], but these materials are not usually considered practical for a commercial process. If there is insufficient oxygen then hydrogen may be formed on the cathode by electro-reduction of water in reaction 3. In a diaphragm cell fed with a single electrolyte the primary anode reaction 4 competes with the destruction of peroxide by the kinetically fast reaction 5. As peroxide accumulates in the electrolyte the selectivity for reaction 4 is maintained by the presence of the micro-porous diaphragm, which suppresses transport of perhydroxyl to the anode by virtue of the ca. 4/1 ratio of diffusivity of OH^- vs. HO_2^-. Perhydroxyl ions also undergo thermal decomposition by reaction 6, which reduces the Faradaic efficiency for net peroxide production.

Table 1. Reactions in electro-synthesis of alkaline peroxide

Reaction	E_e^0 /V vs. NHE at 298 K (pH = 14)	
Cathode		
$O_2 + H_2O + 2e^- \Rightarrow OH^- + HO_2^-$	−0.076	1
$HO_2^- + H_2O + 2e^- \Rightarrow 3OH^-$	+0.878	2
$2H_2O + 2e^- \Rightarrow H_2 + 2OH^-$	−0.830	3
Anode		
$O_2 + 2H_2O + 4e^- \Leftarrow 4OH^-$	+0.401	4
$O_2 + H_2O + 2e^- \Leftarrow OH^- + HO_2^-$	−0.076	5
Bulk		
$2HO_2^- \Rightarrow 2OH^- + O_2$	–	6

The overall reaction in alkaline solutions, derived by subtracting 0.5 times reaction 5 from reaction 1, is:

$$0.5O_2 + OH^- \Rightarrow HO_2^- \quad (1)$$

or subsequently the HO_2^- may be speciated by Na^+ to give alkaline peroxide:

$$Na^+ + HO_2^- \Rightarrow NaHO_2 \quad (2)$$

In conventional reactors for the electro-synthesis of alkaline peroxide, oxygen generated at the anode is collected and recycled to the cathode via an external process loop. In contrast, the design of the perforated bipole reactor allows oxygen from each anode to flow directly through the electrode perforations into the adjacent cathode. The porous diaphragm, coupled with direct communication between adjacent cells in the bipolar stack, also allows the perforated bipole reactor to operate at super-atmospheric pressure to support a high mass transport limiting current density for oxygen reduction.

A practical perforated bipole continuous reactor contains multiple cells connected in series for current and manifolded in parallel for 2-phase (gas/liquid) fluid flow. Difficulties that arise with this unconventional reactor design are mostly related to internal current by-pass through the bipole perforations and the inter-cell manifold, plus the mal-distribution of the reactant fluids between the cells. Also, since the reactor operates under nearly adiabatic conditions, Joule heating can raise the electrolyte temperature to the point (e.g. > 70 °C) where peroxide loss by the homogeneous reaction 6 is a major concern [8, 14].

3. Experimental

Figure 1 shows the process flow diagram used in the present work for the electro-synthesis of alkaline peroxide solutions. In this process oxygen gas from a cylinder and aqueous sodium hydroxide solution from a pump were metered, combined at a tee and delivered in 2-phase flow to the bottom of the electrochemical reactor. The product alkaline peroxide solution and excess oxygen from the top of the reactor passed through a cooler and pressure control valve (PC) to a gas/liquid separator, from which the excess oxygen was vented and the peroxide solution delivered to a product tank.

The pressures and temperatures in the process were monitored by gauges and thermometers at the reactor inlet and outlet. Power was supplied to the reactor in the galvanostatic mode from a 30 A DC supply, and the

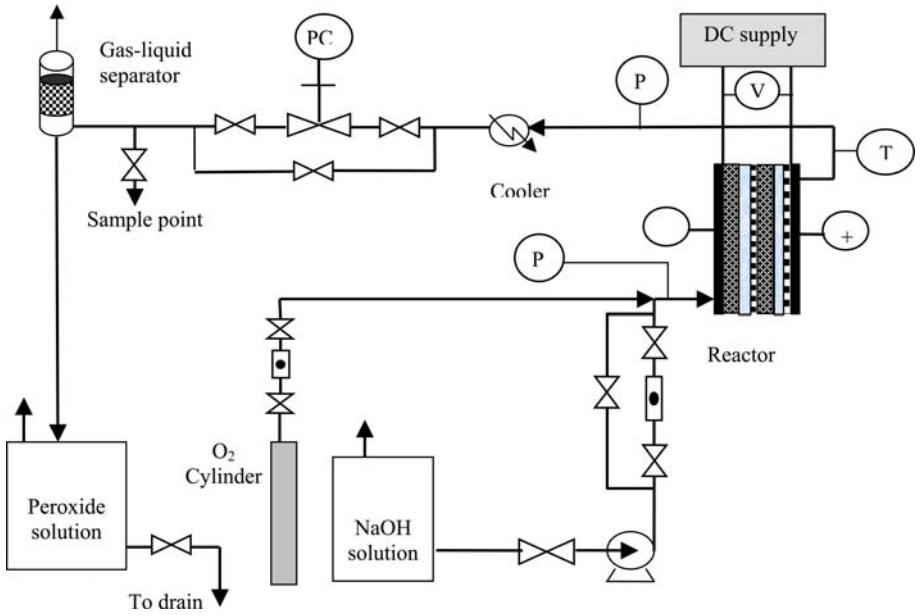

Fig. 1. Process flow diagram.

current and reactor voltage monitored respectively by an in-line ammeter (A) and a voltmeter (V) across the reactor terminals. The peroxide product was withdrawn periodically from the sample point and analyzed for peroxide concentration by titrating the acidified solution with potassium permanganate [18].

The reactor described in Figure 1 may be a single, two or multiple cell reactor. The single- and two-cell configurations are described below.

3.1. *Reactor configuration*

Figure 2 shows the configuration of the single-cell reactor in which the graphite felt cathode (6) is fitted into the Durabla (asbestos based) gasket (5) followed by a separator (diaphragm (7)), nickel mesh anode (8), perforated Grafoil anode (9) and a nickel mesh dummy anode (10) fitted between the feeder cathode (3) backed with Grafoil sheet (4) and feeder anode (11). The dummy anode is electronically shorted to the feeder anode and allows the oxygen generated at the end anode to disengage from the anode and leave the reactor. The whole assembly is tightly fitted between two carbon steel channels (1) and (13) and insulated from the feeder plates (3 & 11) using Durabla gaskets (2 & 12) to form a filter press type of cell. Current is supplied to the reactor through the stainless steel (SS) current feeders (3 & 11) backed with copper plates (not shown). Stainless steel

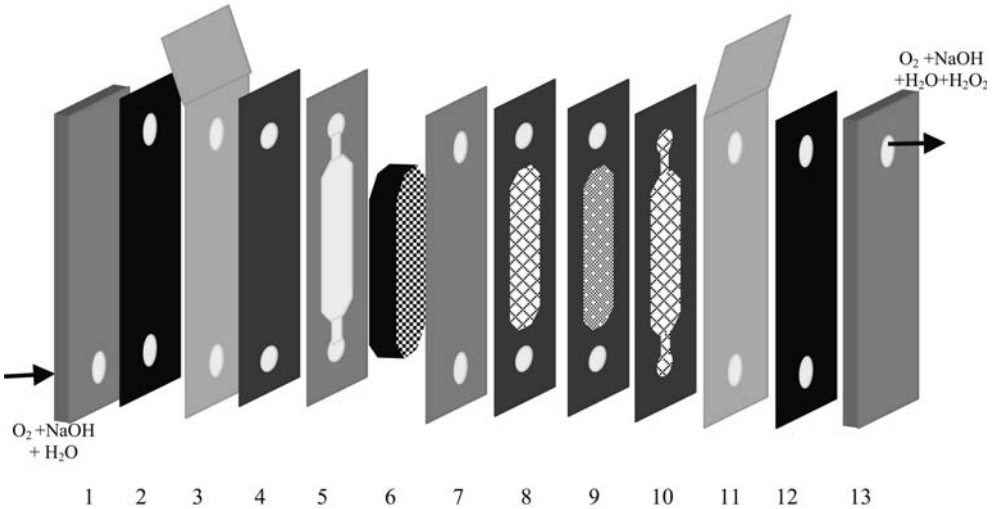

Fig. 2. Single-cell reactor assembly.

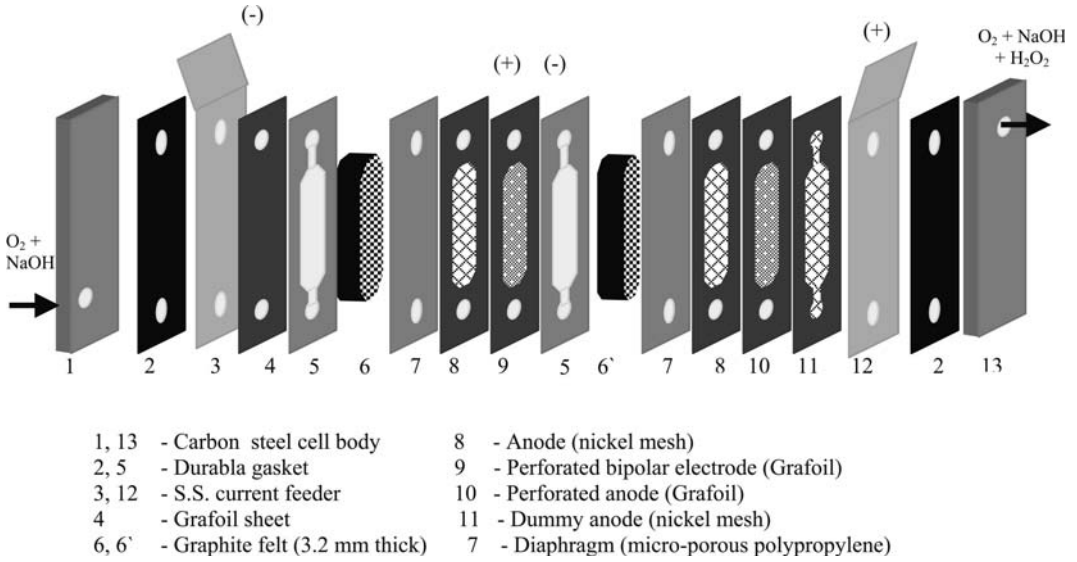

Fig. 3. Two-cell reactor assembly.

couplings (not shown) welded into the SS current feeders serve as the fluid feed and product ports.

The two-cell assembly in Figure 3 is similar to the single-cell assembly of Figure 2, except that the two cells are adjacent to one another in electrical series. The central perforated Grafoil sheet (9) is a bipolar electrode. It behaves as an anode on one side and a cathode feeder on the other, and allows oxygen gas generated on the anode (8) to flow into the adjacent cathode (6′).

The active dimensions in both the single- and two-cell reactors are those shown in Figure 4, i.e. 120 mm high by 25 mm wide, with the graphite felt cathode compressed from 6.4 mm and 95% porosity to a thickness of 3.2 mm and about 90% porosity.

3.2. *Reactor components*

A key aspect of the design of the perforated bipole peroxide reactor is the selection of the configuration and materials of the anode/bipole, cathode and diaphragm that are illustrated in the cell section of Figure 5. The properties of these coupled cell components are critical to the reactor performance.

3.2.1. *Anode/bipole*

The issue of the anode/bipolar selection may be approached by considering the generation and disengagement of oxygen gas in the cell section of Figure 5.

Oxygen is generated at the anode (C) at a rate proportional to the current density for reactions (4) and (5) and must be disengaged to prevent blinding the anode surface. The capillary pressure in the microporous hydrophilic diaphragm (B) prevents the anode gas from flowing into the primary cathode (A) but perforations in the bipole (D) allow the oxygen to disengage into the adjacent cathode (E), or into the dummy anode of the terminal cell of the bipole stack. The bipole perforations that allow gas to disengage from the anode also provide a path for current bypass through the bipole plate, with a consequent loss of Faradaic efficiency of the process. Further, at high current density (e.g. >2 kA m^{-2}) gas accumulation on the anode can result in mal-distribution of the current, causing corrosion and local overheating that may ''burn out'' the diaphragm and short the cell. The problems of current by-pass and cell ''burn out'' are handled by balancing the rate of oxygen generation against the thickness and porosity of the anode, together with the size and coverage of the bipole perforations – with the aim to have the bipole perforations loaded with gas (i.e. electrolyte free) during reactor operation.

Materials tested for the anode (C) and bipole plate (D) in the initial experiments were:

ANODE: Plain stainless steel mesh (200 mesh/inch), plain nickel mesh (40,50 and 100 mesh/inch from Argus Inc. Virginia U.S.A.), plasma sprayed Raney (porous) nickel, plasma sprayed Raney (porous) nickel on nickel mesh, electro-less nickel on nickel mesh, electro-less nickel on stainless steel mesh.

BIPOLE: Grafoil[1] (1.6 mm thick), stainless steel (1.6 mm thick).

The uniformly distributed circular perforations in the bipole plate were specified by their diameter and coverage, where coverage is defined as:

Coverage = total area of perforations/superficial area of active bipole

The values of these critical variables were established in previous experiments (not described here) and ranged respectively from 0.5 to 1.6 mm and 1–5%.

Of the materials listed above nickel was selected for its relative stability and low over-voltage for anodic oxygen

[1] Grafoil is a compressed graphite sheet with stainless steel insert, purchased from Union Carbide Corp. of New Jersey, U.S.A.

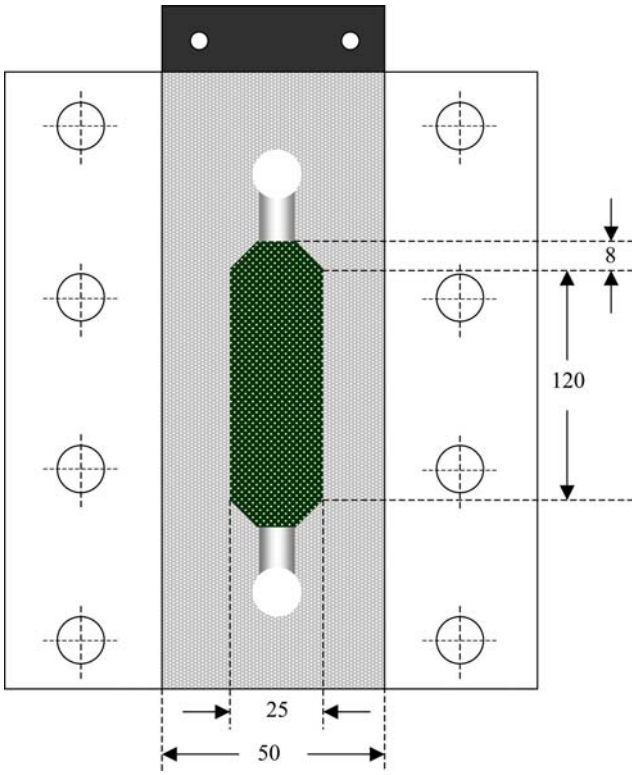

Fig. 4. Cathode configuration (dimensions in mm).

generation in alkali, while Grafoil was chosen for two reasons:

(a) The kinetics of oxygen and peroxide reduction [17] make graphite the preferred material for the cathode feeder in the adjacent cell (i.e. cathode E in Figure 5). This arrangement should allow peroxide to be produced rather than be destroyed by any residual Faradaic current on the cathode feeder.

(b) The required perforations are easily made in the laboratory by punching the soft Grafoil material.

Subsequent experiments were also conducted on a novel compound bipole electrode, aimed to eliminate current bypass through the bipole perforations.

This novel compound bipole consisted of two sheets of porous PTFE sandwiched between 3 sheets of perforated Grafoil as shown in Figure 6, in which the perforations in the central Grafoil sheet (diameter 1.6 mm, 2% perforation coverage) are filled with 0.5 mm diameter polystyrene beads.

3.2.2. *Diaphragm*

The diaphragm separator (item B in Figure 5) is a critical component of the reactor and has three purposes:

(1) To prevent electrical short circuit between the primary cathode (A) and the anode (C) in each cell of the in the filter press reactor.

(2) To maintain a high positive capillary pressure that prevents penetration by gas produced at the anode. This requirement implies a hydrophilic material with a pore size in the micron or sub-micron range.

(3) To suppress the transport of perhydroxyl ions from the primary cathode (A) to the anode (C).

Regarding item 3 the diaphragm (a.k.a. separator) properties should be considered with respect to the

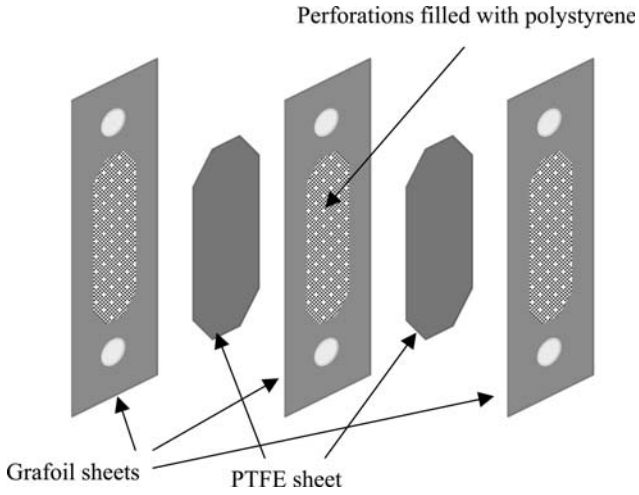

Fig. 6. Novel bipolar electrode.

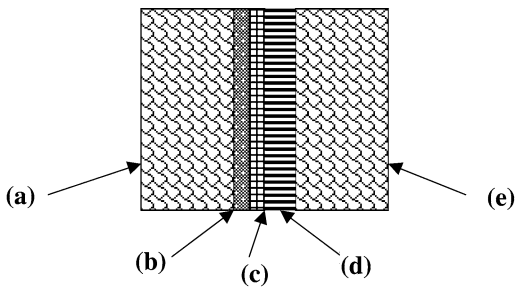

(a) = graphite felt cathode **(b)** = micro-porous hydrophillic diaphragm

(c) = porous anode (e.g. nickel mesh) **(d)** = perforated bipole (e.g. punched Grafoil sheet)

(e) = adjacent graphite felt cathode

Fig. 5. Cell section in a perforated bipole reactor.

competitive transport of OH^- and HO_2^- to the anode by diffusion, migration and convection, of which convection is the major source of peroxide loss to the anode. The convective transport is dependent on the thickness, tortuosity and porosity of the diaphragm. The thicker, more tortuous and less porous the diaphragm, the lower the convective flux. However increased thickness and tortuosity and decreased porosity cause an increase in the electrical resistance of the diaphragm, with relatively higher specific energies for peroxide generation. Selection of the diaphragm thus involves a trade-off between convective electrolyte flow and conductivity.

Previous experience at U.B.C. (including tests with cation and anion exchange membrane separators) has identified hydrophilic micro-porous polyolefin as an acceptable separator material. Some properties of two such materials found suitable and used in the present work are summarized in Table 2.

3.2.3. *Cathode*

The properties of the 3D carbon cathode are central to electro-synthesis of alkaline peroxide and there are many forms of carbon that could be used here.

Past experience at U.B.C. with active carbon, crushed petroleum graphite, carbon black in PVC, reticulated carbon and carbon fibre mat or felt has shown carbon (graphite) felt to be superior to the other materials. Teflonated carbons, such as that used by H-D Tech [10] and that described by Sudoh et al. [12] may also be useful here, but have not been studied at U.B.C. In the present work graphite felt was chosen as the cathode material because of its high porosity and specific surface area, together with the ease of fabricating large electrodes (i.e. >0.01 m^2 superficial area) from commercially available felts. The felt was obtained from Metaullics Systems Inc. (previously Carborundum), Sanborn, NY U.S.A. and has the properties listed in Table 3.

The configuration of each cathode (items A and E in Figure 5) is shown in Figure 4. The graphite felts were prepared by immersion in 5 wt% nitric acid at 20 °C for 24 h to remove any metal ion contaminants. A wetting agent, Makon-12, ($0.002\%_w$) was added to the nitric acid solution to make the felt wettable.

3.3. *Electrolyte additives*

Previous studies at U.B.C. have shown that the presence of trace amounts of iron, manganese and other transition metals in the reactor feed cause an increased voltage and decreased current efficiency for peroxide in long term operation of the reactor. To overcome this problem complexing agents may be added to the feed to chelate the trace metal ions [20].

In the present work DTPA (diethylenetriaminepentaacetic acid, sodium salt) in the concentration [$0.002\%_w$] was added to the reactor feed and is typically available under the trade name "Kalex Penta" from Hart Chemicals, Toronto.

A wetting agent was also added to the reactor feed as a standard practice to keep the diaphragm (polypropylene separator) wetted by the electrolyte. The usual addition was $0.002\%_w$ of Makon NF12, a low foaming polyoxyethylene alcohol from Stepan Chemical Co. U.S.A.

3.4. *Experimental conditions*

The experimental conditions of this work are summarized in Table 4.

4. Results and discussion

4.1. *Anode/bipole*

Figure 7 shows the peroxide current efficiency and specific electrical energy consumption for peroxide generation measured in tests on various anode/bipole combinations in the single-cell reactor under the conditions listed in Table 4. These results reflect a wide range of reactor performance and highlight the importance of the anode/bipole design to reduce current bypass and promote the disengagement of oxygen.

Figure 7 indicates that in operation near atmospheric pressure the perforated bipole peroxide reactor can give reasonable performance with superficial current density up to 6 kA m^{-2}. The trend of decreasing peroxide

Table 2. Diaphragm properties

Source	Material	Type	Thickness mm	Porosity /%	Basis weight /g m^{-2}	Ion exchange capacity /meq g m^{-1}	Electrolyte absorption /g m^{-2}	Wicking rate[b] /mm/600 s
PALL RAI Inc. U.S.A.[a]	Radiation grafted polypropylene	PHDC 120	0.5	85	na	na	na	na
SCIMAT Ltd. U.K.	Micro-porous polypropylene	700/20	0.15	na	45	0.6	>140	>70
		700/25	0.22	na	72	0.8	>140	>50
		700/28	0.29	na	85	0.6	>190	>50
		700/29	0.12	na	38	0.6	>120	>70
		700/74	0.18	na	60	0.8	>75	>75

[a]Now defunct. [b]Measured in 30 wt% aqueous KOH at 24 °C.

Table 3. Cathode properties

Property	Value	Source
Initial porosity, ε_0	0.95	Metaullics systems Inc.
Mean fibre diameter (μm), d_f	20	Idem
Fibre density (kg m^{-3})	1500	Idem
Graphitization (°C h^{-1})	2400/2	Idem
Carbon content (%)	99	Idem
Uncompressed thickness (mm), t_0	6.4	Metaullics systems Inc.
Compressed thickness (mm), t	3.2	Measured
Compressed porosity, ε	0.90	Measured
Compressed specific surface area (m^{-1}), s	20 000	$\varepsilon = 1 - t_0(1-\varepsilon_0)/t$
Electronic conductivity of compressed matrix (S m^{-1}), k_{aps}	39.2	$s = 4(1-\varepsilon)/d_f$ $k_{aps} = 10 + 2800(1-\varepsilon/\varepsilon_0)^{1.55}$ [Oloman et al., 19]

Source: (Type Grade GF, Metaullics Systems Inc.)

Table 4. Experimental conditions

Experiment →		Anode/bipole Figure 7	Diaphragm Figure 8	Cells Figures 9, 10	Compound bipole Figure 11
NaOH conc.	M	1.0	1.0	1.0	1.0
NaOH flow	ml/min/cell	20	20	20	20
O_2 flow	ml STP/min/cell	200	200	200	200
Reactor pressure	kPa (abs) in–out	125–100	125–100	800–775	900–875
Reactor Temperature	°C in–out	20–45 °C	20–45 °C	20–45 °C	20–45 °C
Anode/bipole		Various	Ni 100#/Grafoil	Ni 100#/Grafoil	Ni 100#/Grafoil PTFE/PS
Bipole perforation	diam mm/coverage %	Various	1.6/4	1.6/2	1.6/2
Diaphragm type		RAI PHDC 120	Various	SCIMAT 700/20	SCIMAT 700/20
Cathode	Thickness mm/porosity %	Graphite felt 3.2/90	Graphite felt 3.2/90	Graphite felt 3.2/90	Graphite felt 3.2/90
No. of cells		1	1	1 and 2	2

current efficiency with increasing superficial current density is largely due to increased local over-potential in the graphite felt cathode that promotes the secondary reaction 2 over the mass transfer constrained reaction 1. The increase of specific energy with current density is a result of the combined effects of decreasing current efficiency and the increasing cell voltage (cf. the voltage balance) that is caused, in part, by increased gas hold-up in the anode.

Of the various meshes selected to provide sufficient anode surface for electrolyte contacting, it was found that Ni mesh (40#), Ni mesh (100#) and Ni mesh (100#) coated with porous nickel gave the best results in terms of high current efficiency with low specific energy, Cells using Ni mesh (40#) and Ni mesh (100#) anodes gave lower specific energies than nickel mesh (100#) coated with porous nickel. Uncoated nickel mesh (100#) was chosen as the anode material in subsequent experiments because it was cheaper than nickel mesh (40#).

Figure 7 shows that Raney nickel-based anodes gave significant benefit in terms of the specific energy; with current efficiency similar to that of the nickel mesh. However the cost (in time and money) of fabricating these anodes in the laboratory was prohibitive so they were not investigated further in the current work.

4.2. *Diaphragm*

Figure 8 shows the current efficiency and specific energy consumption measured in tests on various diaphragms in the single-cell reactor under the conditions listed in Table 4.

These plots indicate that SCIMAT 700/20 is the best material here, as the current efficiency, in the current density range of importance 3–5 kA m^{-2}, is the highest and specific electrical energy consumption the least. This material also appeared to be stable over the operating time of the experiments (e.g. several hours). Therefore SCIMAT 700/20 was chosen as the diaphragm material for subsequent work.

4.3. *Two-cell reactor*

Figures 9 and 10 show results of experimental runs on single- and two-cell reactors under the conditions listed in Table 4. These reactors were operated under super-atmospheric oxygen pressure (ca. 800 kPa (abs)) and thus gave superior performance to that reported in Figure 7 and 8.

Figure 9 shows that peroxide can be generated in the single-cell reactor at concentrations up to 0.15 M in 1 M NaOH with ca. 65% peroxide current efficiency at a superficial current density of 5 kA m^{-2}, corresponding to a partial current density for reaction 1 of about 5 kA m^{-2}.

Figure 9 also shows that the peroxide current efficiency in a two-cell reactor is significantly lower than that in a single-cell reactor, while the specific electrical energy consumption for peroxide generation (Figure 10) is slightly higher than that in the single cell case. These

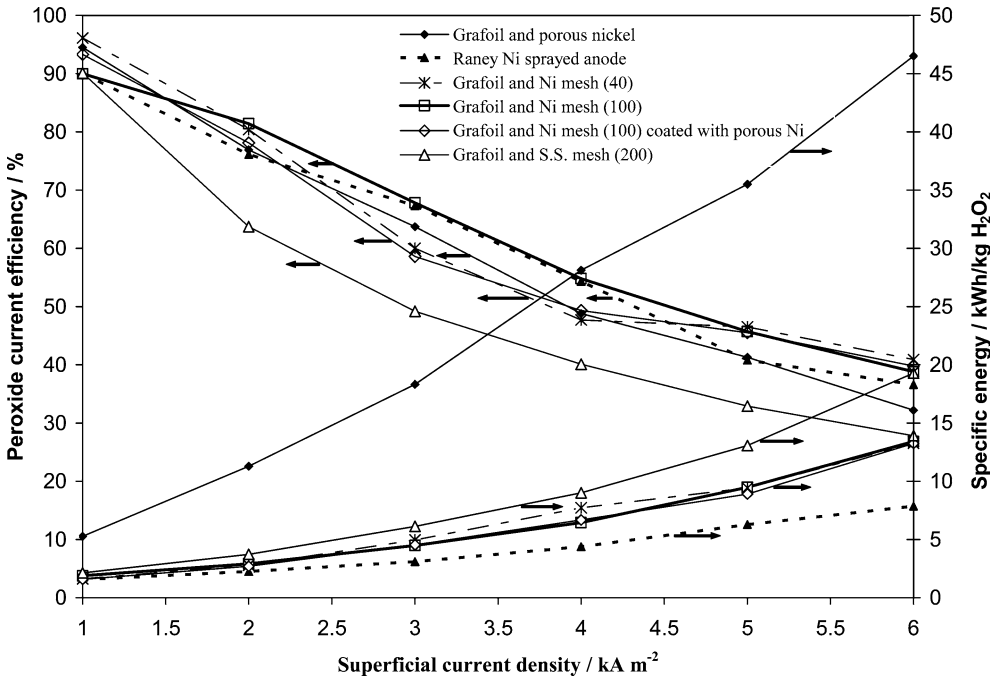

Fig. 7. Peroxide current efficiency and specific electrical energy consumption for peroxide generation vs. superficial current density for different anodes in the single-cell reactor.

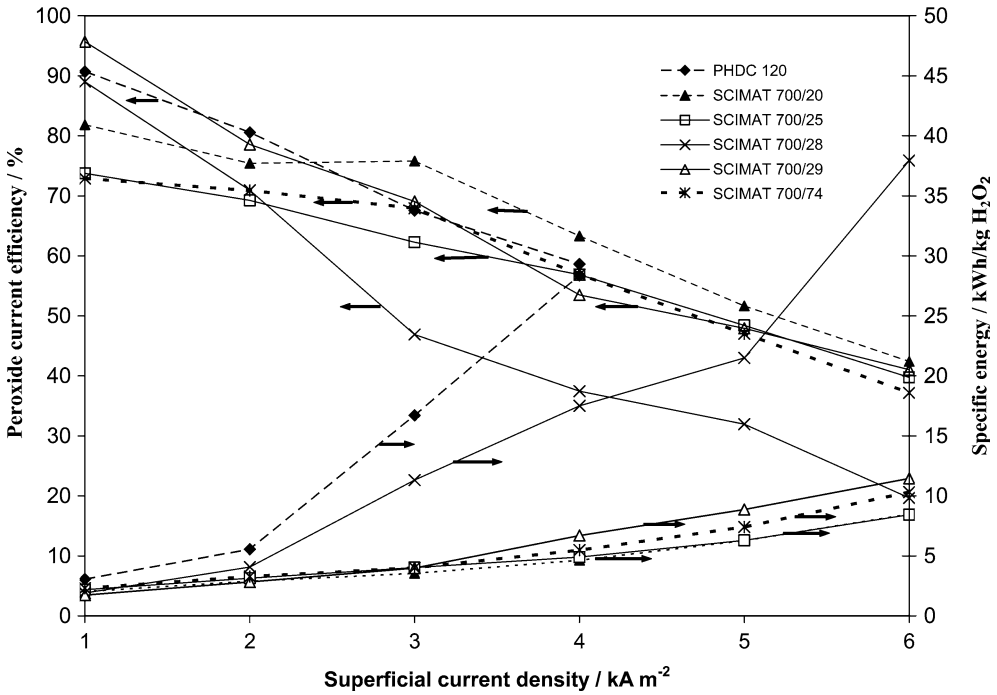

Fig. 8. Peroxide current efficiency and specific electrical energy consumption for peroxide generation vs. superficial current density for different diaphragms in the single-cell reactor

effects are primarily due to current bypass in the two-cell reactor that decreases both the peroxide current efficiency and the individual cell voltages.

4.4. *Compound bipole*

Figure 11 show results of experimental runs with the compound bipole in a two-cell reactor under the conditions listed in Table 4. Here it can be seen that the current efficiency for the two-cell reactor using a PTFE-based bipole (Figure 6) is substantially higher, while the specific energy is lower, than the corresponding values without the PTFE inserts. The difference between the two types of bipole (with and without PTFE inserts) decreases with increasing current density due to a corresponding increased ratio of Faradaic to bypass current.

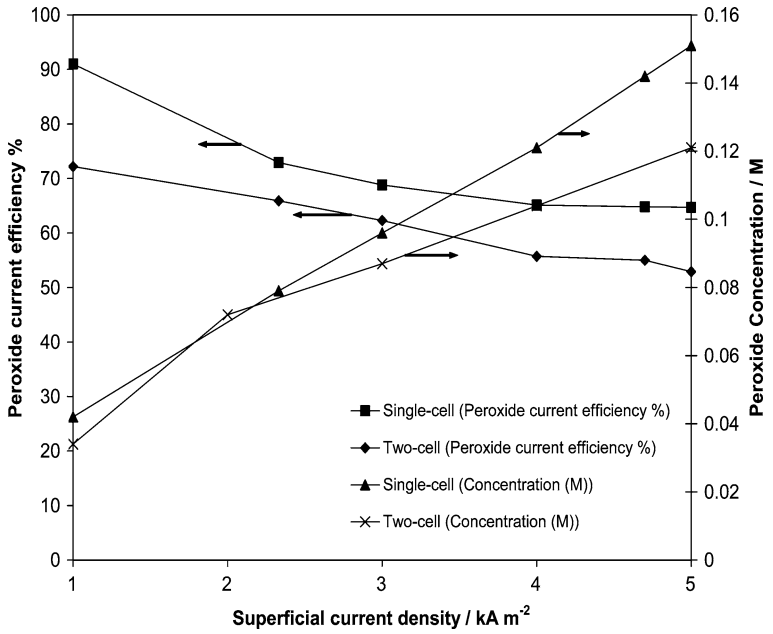

Fig. 9. Peroxide current efficiency and peroxide concentration vs. superficial current density for single- and two-cell reactor

In essence, the use of a PTFE-based bipolar electrode improves the performance of the reactor significantly, presumably by reducing the current bypass due to electrolyte while allowing the gas to disengage from the anode. Such electrodes could find future use in a scaled-up reactor for alkaline peroxide production and may offer a solution in other industrial electrochemical systems where gas disengagement from bipole electrode is required.

5. Conclusions

Alkaline peroxide was generated in a novel perforated bipolar trickle-bed electrochemical reactor with superficial electrode dimensions 120 mm high by 25 mm wide with a 3.2 mm thick cathode. The two-cell reactor showed good performance for production of peroxide at current densities from 2 to 5 kA m^{-2}, with current efficiency and specific energy respectively in the range 78–50% and 4.5–9 kWh per kg H_2O_2 and peroxide concentrations in the range 0.07–0.15 M in 1 M NaOH.

Various electrode and diaphragm materials were tried to select suitable components for the present work. It was found that nickel mesh (100#) in conjunction with perforated Grafoil and micro-porous polypropylene sheet served as a useful anode/bipole/diaphgram combination that could be easily fabricated in the laboratory and gave good performance in experimental runs of several hours.

In conjunction with the anode/bipole of this work a new bipole was invented that could substantially lower

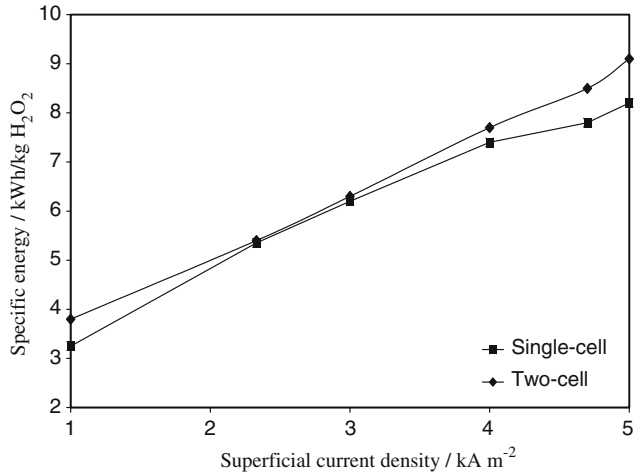

Fig. 10. Specific electrical energy consumption for peroxide generation vs. superficial current density for single- and two-cell reactor.

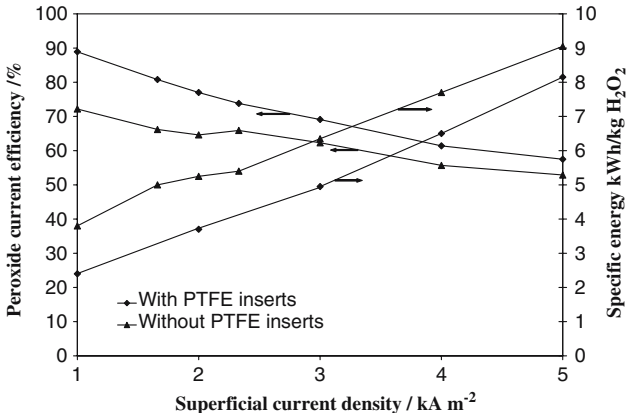

Fig. 11. Peroxide current efficiency and specific electrical energy consumption for peroxide generation vs. current density for two-cell reactor with bipolar electrode with and without PTFE inserts.

the current bypass in the bipole reactor. The bipole used three perforated Grafoil sheets with hydrophobic inserts/filling to prevent electrolyte loading the perforations. This novel bipolar electrode may be used in other industrial bipolar electrochemical reactors where gas generation at one of the electrodes is an issue.

Work on the scale-up and modeling of the perforated bipole trickle-bed electrochemical reactor will be described in subsequent publications.

Acknowledgements

This work was supported by grants from the Government of Canada through the Natural Science and Engineering Research Council (NSERC) and the "Wood Pulps" Network of Centre of Excellence, with facilities supplied by the University of British Columbia (U.B.C.) and the U.B.C. Pulp and Paper Centre.

6. Appendix

Following terms used in the paper are described here:

Superficial current density: Current per unit surface area of the planar electrode (i.e. 32 cm^2 in the present electrochemical system cf. Figure 4)

Real current density: Current per unit real surface area of the 3D graphite electrode (20 000 m^2/m^3 of felt volume in the present electrochemical system).

Peroxide current efficiency: Peroxide current efficiency is defined as the percentage of the total current that goes in to generate peroxide

The current efficiency in a complete bipolar electrochemical reactor for a particular product is given by:

$$\mathrm{CE} = \frac{n_0 F(\text{product rate})}{n_{\text{cell}} I_{\text{reactor}}} \qquad (A.1)$$

where F is the Faraday constant (96 486 C mol^{-1}) I_{reactor} is the total current fed to the reactor, Amperes and n_{cell} is the number of cells in the reactor and product rate in mol s^{-1}.

The peroxide current efficiency is based on Equation (A.1) and is given by:

$$\mathrm{CE} = \frac{2000 F C_{\mathrm{HO2-}}(v_{\text{elec}})}{n_{\text{cell}} I_{\text{reactor}}} \qquad (A.2)$$

where $C_{\mathrm{HO2-}}$ is the peroxide concentration exiting the reactor, kmol m^{-3}, v_{elec} is the electrolyte flow rate in the reactor, m^3 s^{-1}, I_{reactor} is the total current fed to the reactor, Amperes and n_{cell} is the number of cells in the bipolar reactor.

Specific electrical energy consumption:

The specific energy for product generation (kWh kg^{-1} product) is given by:

$$\mathrm{SE} = \frac{n_0 F |V_{\text{cell}}|}{n_{\text{cell}}(3600)\mathrm{MW}_{\text{product}}(\mathrm{CE})} \qquad (A.3)$$

where n_0 is the number of electrons taking part in the reaction to produce the given product, V_{cell} is the cell voltage $\mathrm{MW}_{\text{product}}$ is the molecular weight of the product in kg $kmol^{-1}$.

The specific energy for peroxide generation (kWh kg^{-1} H_2O_2) is given by:

$$\mathrm{SE} = \frac{2F|V_{\mathrm{r}}|}{n_{\text{cell}}(3600)(34)\mathrm{CE}} \qquad (A.4)$$

where V_{r} is the reactor voltage in V and n_{cell} is the number of cells in the reactor.

References

1. M. Traube, *Chem. Ber.* **15** (1882) 2434.
2. C.W. Dence and D.W. Reeve, *Pulp Bleaching – Principles and Practice* (Tappi Press, Atlanta, Georgia, 1996).
3. C. Oloman, *Electrochemical Processing for the Pulp and Paper Industry* (The Electrochemistry Consultancy, Romsey, UK, 1996).
4. P.C. Foller and R.T. Bombard, *J. Appl. Electrochem.* **41** (1995) 613.
5. E. Berl, *Trans. Electrochem. Soc.* **76** (1939) 359.
6. P.C. Foller et al. *The use of gas diffusion electrodes in the on-site generation of oxidants and reductants*, Fifth Int. Forum on Electrolysis in the Chemical Industry. Ft. Lauderdale. Nov. (1991).
7. T.S. Drackett, US Pat. No. 5358609 (1994).
8. C. Oloman and A.P. Watkinson, *J. Appl. Electrochem.* **9** (1979) 117.
9. J.A. McIntyre and R.F. Phillips, US Pat. 4,406,758 (1983).
10. I.R. Mathur and R. Dawe, *Tappi J.* **82** (1999) 157.
11. Chemical Market Reporter. April (2005).
12. M. Sudoh, M. Yamamoto, T. Kawamoto, K. Okajima and N. Yamada, *Mathematical modeling of trickle-bed cathode with variable wettability for on-site electrochemical production of hydrogen peroxide*, Electrochem. Soc. Proceedings, Electrochem. Soc., New Jersey 99–39 (1999) 207.
13. M. Sudoh, M. Yamamoto, T. Kawamoto, K. Okajima and N. Yamada, *J. Chem. Eng. Japan* **34** (2001) 884.
14. N. Gupta, PhD thesis, University of British Columbia, Vancouver, BC, Canada (2004).
15. I. Hodgson and C. Oloman, *Chem. Eng. Sci.* **54** (1999) 5777.
16. C. Oloman, U.S. Pat. 4,728,409 (1988).
17. K. Kinoshita, *Electrochemical Oxygen Technology* (John Wiley & Sons, New York, 1992).
18. A.I. Vogel, *A Text Book of Quantitative Inorganic Analysis* (Longmans, New York, 1978).
19. C. Oloman, M. Matte and C. Lum, *J. Electrochem. Soc.* **8** (1991) 2330.
20. C. Oloman, Can. Pat. 1214747 (1986).